Int. J. Electrochem. Sci., 13 **(2018)** 1062 – 1073, doi: 10.20964/2018.01.86

International Journal of
ELECTROCHEMICAL
SCIENCE
www.electrochemsci.org

Electrochemical Noise Analysis of Corrosion Behavior of Stainless Steel 304 Exposed in NaCl and $FeCl_3$ solutions.

A. Mandujano-Ruíz[1,*], *J. Morales-Hernández*[1], *F. Castañeda-Saldivar*[1], *H. Herrera-Hernández*[2], *J.M. Juárez- García*[3]

[1] Centro de Investigación y Desarrollo Tecnológico en Electroquímica (CIDETEQ), Parque Tecnológico Querétaro s/n, Sanfadila Pedro Escobedo, Querétaro, C.P. 76703, México.
[2] Universidad Autónoma del Estado de México, IIN-Lab. de Electroquímica Aplicada y Corrosión de Materiales Industriales, Blvd. Universitario s/n, Atizapán de Zaragoza, Estado de México 54500, México.
[3] Centro Nacional de Metrología (CENAM), Km 10 carretera los Cués, El Márquez, Querétaro, C.P. 76703, México
[*]E-mail: amandujano@cideteq.mx

Received: 27 September 2017 / *Accepted:* 7 November 2017 / *Published:* 16 December 2017

Electrical parameters such as charge of the event (q), characteristic frequency (f_n) and impedance (Z_n) obtained from shot-noise theory have been proposed as indicators of the initiation of pitting corrosion, and have played an important role in the construction of corrosion patterns which are a good approximation to examine the evolution of corrosion type in metals and its alloys. Therefore, in this research paper, Electrochemical Noise (EN) signals (potential and current noise data) have been collected from AISI 304 stainless steel exposed to chloride solution to evaluate the pitting corrosion behavior. The electrochemical tests were carried out at standard condition during 24 hours of exposure in two chlorine solutions (NaCl and $FeCl_3$). Noise data analysis was mathematical treated by wavelet transform in order to identify the low frequencies that lead the calculation of q, f_n, and Z_n to plot the corrosion behavior and this was correlated with the Energy Distribution Plots (EDP) and metallographic images. The results of all the time series evaluated reveals a concordance in scale of EDP with the initiation and the growth of pitting.

Keywords: Electrochemical noise, Pitting corrosion, Wavelet Transform, Energy Distribution Plot, 304SS.

1. INTRODUCTION

Electrochemical Noise (EN) is known since its introduction in the 60's with the first records of fluctuation in potential obtained during the iron corrosion [1]. Later, thanks to the incorporation of zero resistance ammeter (ZRA), the record of fluctuation in current was possible, so that, EN was then

identified as a novel technique for corrosion monitoring. The main advantage of EN against other electrochemical techniques like Electrochemical Impedance Spectroscopy (EIS) or Linear Polarization Resistance (LPR), is the facility to obtain information of the system without an external perturbation [2-4]. Nowadays, EN signals have contributed to the study of several phenomena such as nucleation, meta-stable pit [5] and its growth [6], crevice and general corrosion, formation of passive films or oxide layers [7, 8], inhibition mechanism [9], generation and propagation of cracks under stress at different temperatures [10-16], among others. Once the EN data are recorded, the next step is the selection of an appropriate mathematical method to obtain enough information from the signal and, get the best interpretation of the phenomenon. Compilation of methodologies for the processing of EN signals involves three fundamental aspects: *i*) the analysis of the Temporal Domain that consider the statistical treatment and theories like shot noise; *ii*) the analysis of the Frequency Domain (Discrete Fourier Transform, ***DFT***) and, *iii*) the combination of both domains Time-Frequency (Wavelet Transform, ***WT***); being the last one of great interest for its advantage of separating a group of frequencies and knowing its occurrence time [11, 17-19]. Each of these methodologies provides energetic parameters that allow to classify the high frequency signals related with the passivation process or uniform corrosion state; while the low frequency are related with pitting corrosion mechanism; thus allowing the monitoring of the corrosion evolution in the metal [20, 21].

Energetic parameters can be enhanced by the use of predominance diagrams, which describe the corrosion type and the rate at which it occurs. Examples of these plots are shown in the research work of Al-Mazedi and Cottis [21, 22], who compared several parameters such as the skew in potential and current signals, location index (*IL*), coefficient of variation (CV), charge of the event (q), the frequency of the event (f_n), and the noise resistance (R_n). The last three are the most representative to discriminate the corrosion types (uniform, localized and inhibition) of a carbon steel in CO_2/NaCl/Thioacetamide at different concentrations. Subsequently Cottis [23] followed this study after, incorporating an aluminum alloy exposed to different media, whose predominance diagrams combined parameters of the shot noise theory (q, f_n, and Z_n), resulting good indicators of the corrosion type. In recent studies, Jian Li [24] conducted a research about the effect of temperature on the sensitivity of pitting corrosion in stainless steel 304, demonstrating that the implementation of these diagrams is very useful in monitoring this phenomenon.

In this context, the present work shows the corrosion behavior for a stainless steel 304 exposed in two chlorinated media ($FeCl_3$ and NaCl) where localized corrosion has been previously reported. Denoting that the parameters for the construction of the predominance diagrams were obtained from the shot noise theory and, incorporating an analysis of the signals with the wavelet transform to compare the frequencies in which the onset is presented and evolution of the corrosion mechanism.

2. EXPERIMENTAL DETAILS

2.1 Preparation of test specimen.

A plate of 304SS was mechanically cut to obtain specimens with dimensions of 20x20x5mm;

each specimen was subjected to polish with SiC paper through the numbers 80, 240, 320, 400 and 600 grits until mirror finishing surface with diamond paste of 1 µm. Finally, the specimens were rinsed with distilled water, degreasing with acetone and drying with hot air. The composition of this steel is shown in Table 2.

Table 2. Composition of 304SS

Element	wt%
C	0.08
Mn	2.00
P	0.045
S	0.030
Si	0.75
Cr	18 – 20
Ni	8.0 – 10.5
Fe	Balance

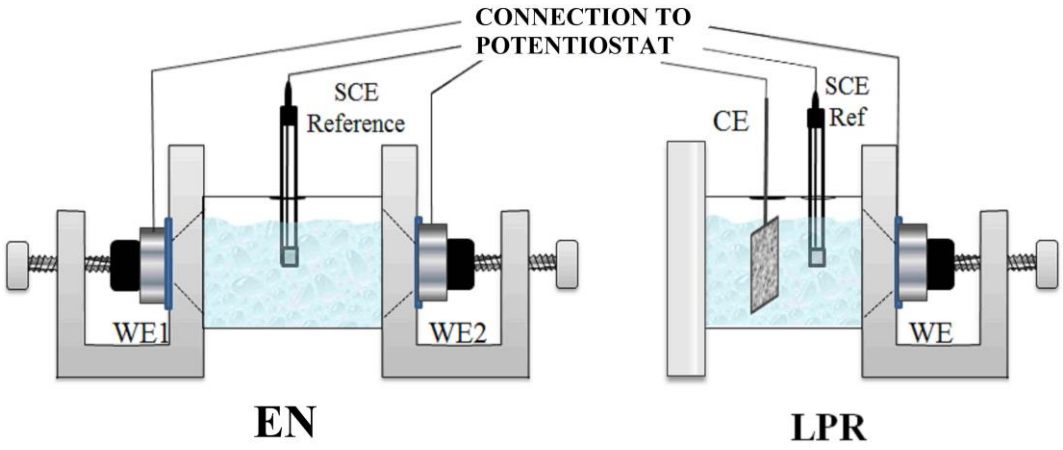

Figure 1. Electrochemical cell arrangement for electrochemical evaluation.

An electrochemical cell for flat specimens was used for Electrochemical Noise Test, the exposition area for working electrodes was 1 cm^2. The arrangement of the cell consists in two identical samples **(WE1** and **WE2)** of 304SS placed as working electrodes in order to register the current noise (ECN) and, a saturated calomel electrode (SCE) as reference was used to monitoring the potential noise (EPN). At the same time, another arrangement was disposed in order to carry out polarization resistance technique (LPR), to obtain the Stern-Geary coefficient (*B)* and the corrosion current (I_{corr}). For this, a typical configuration of three electrodes was set up: 304SS as working electrode WE, platinum mesh as counter electrode (CE) and SCE as reference. A representation of both arrangement on the cell for EN and LPR experiments are shown in Figure 1. To evaluate the development of pitting, two different solutions were used in this research: $FeCl_3$ (0.2 M) and typical NaCl (0.6 M), both of them were prepared with reagent grade salt and distilled water at laboratory conditions.

2.2 Experimental Conditions and Signal Data Treatment

Linear Polarization Resistance (LPR) measurements and Electrochemical Noise (EN) data were achieved in a potentiostat/galvanostat of brand BioLogic® with the use of Ec-Lab software, allowing the configuration of both techniques to be running simultaneously. In the LPR setup, open circuit potential (OCP) was monitored until the system reaches dynamic equilibrium (steady-state condition); after that, a range of ± 25 V was applied for polarization at scan rate of 1 mV/s; this cycle was repeated for 24 hours. In other potentiostat channel, EN measurements were also carried out with the ZRA and with a frequency sampling (f_s) of 2 Hz; duration of each time series was 512 s. From EN data, each time series in current and potential were analyzed by appliying of Discrete Wavelet Transform (DWT) method in Matlab®. The type of wavelet selected was the orthogonal Daubechies grade 4 with 8 levels of resolution, in order to discriminate all the detail coefficients "$d_{1...n}$" included the approximation coefficient "s_8" which content the trend DC in order to remove it from the noise signal. After that, the new signal without trend was processed to obtain the power spectral density (PSD) for both potential and current, allowing to calculate together with the I_{corr} and B, the shot noise parameters such as q, f_n and Z_n in the low frequency domain from the PSD to the final construction of the corrosion diagrams. Parallel to the wavelet decomposition, the coefficients were used to calculate the EDP diagrams. The steps discussed above are illustrated in Figure 2.

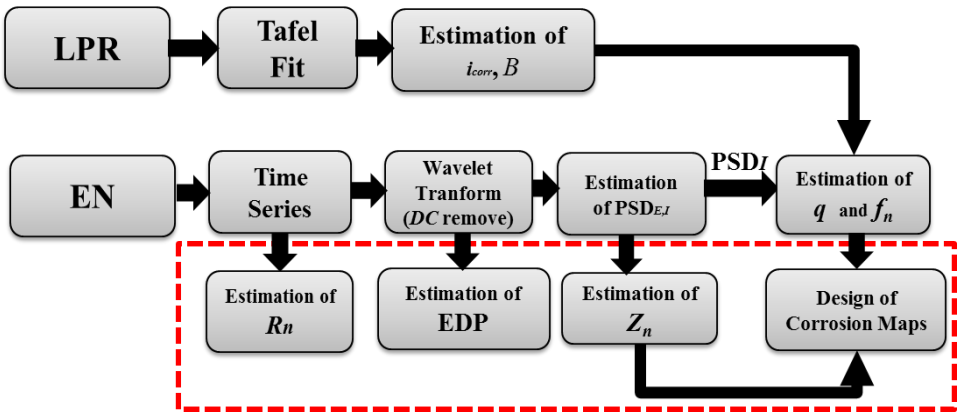

Figure 2. Summary of the methodology used for EN analysis.

3. RESULTS AND DISCUSSION

According with the methodology, Stern-Geary coefficient is the first parameter obtained. The behavior of B along of 24 hours is shown in Figure 3, where the value for both solution ($FeCl_3$ or NaCl) don´t change in magnitude order along the exposure time. However, a greater scattering points was observed for NaCl solution in comparison with $FeCl_3$; this may indicate that the system is

constantly changing to another energy state due to ions charge transfer onto metal interface which modifies the slopes values of b_a (anodic) and b_c (cathodic).

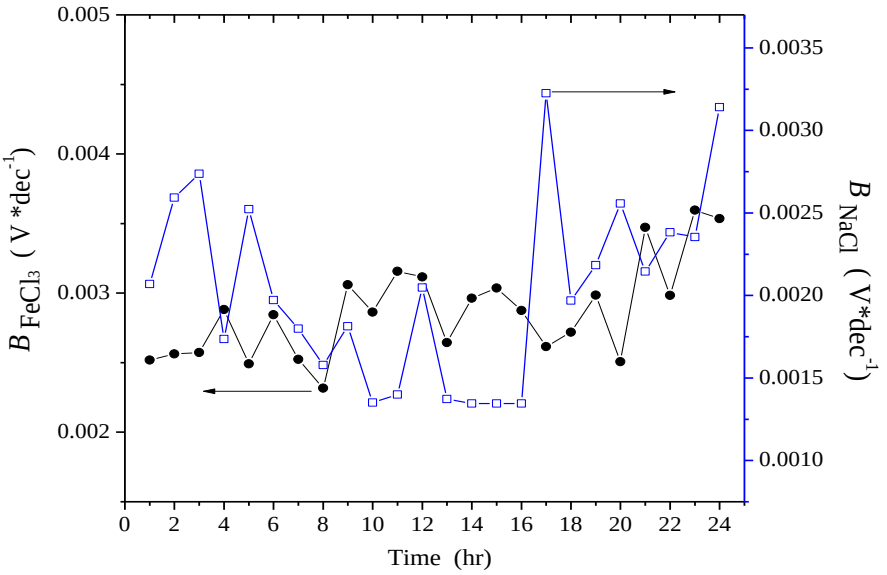

Figure 3. Evolution of *B* coefficient for NaCl and $FeCl_3$ during 24 hours of exposure.

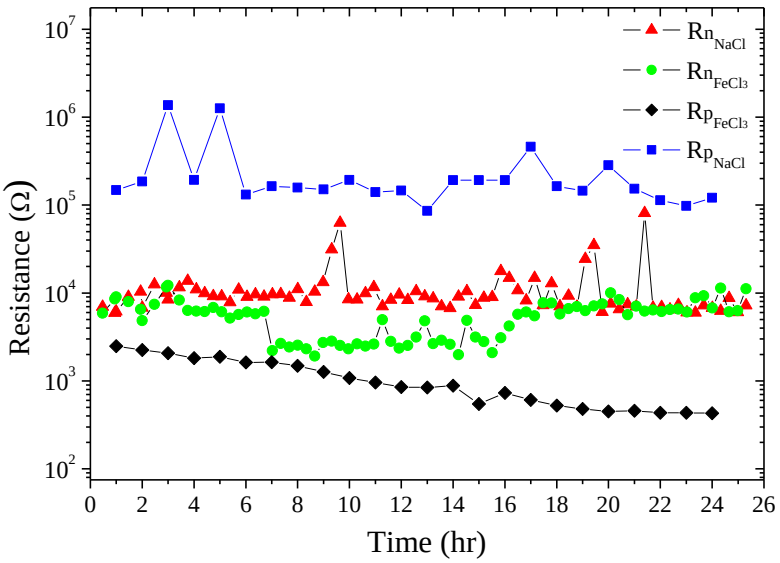

Figure 4. Comparison of R_n and R_p for SS304 in NaCl and $FeCl_3$.

Calculation of *B* and i_{corr} from Tafel fit allows to determine R_p for corrosion rate estimation. R_p is compared with R_n (obtained from noise signals) in Figure 4, where the trending of NaCl for R_n and R_p are above of $FeCl_3$, indicating that SS304 exposed in NaCl is more resistive than $FeCl_3$, whose resistance tends to decrease with respect the exposition time. This behavior was expected due to the presence of oxidizer Fe^{3+} ion that increases the corrosive activity of $FeCl_3$ medium and consequently the corrosion rate is bigger.

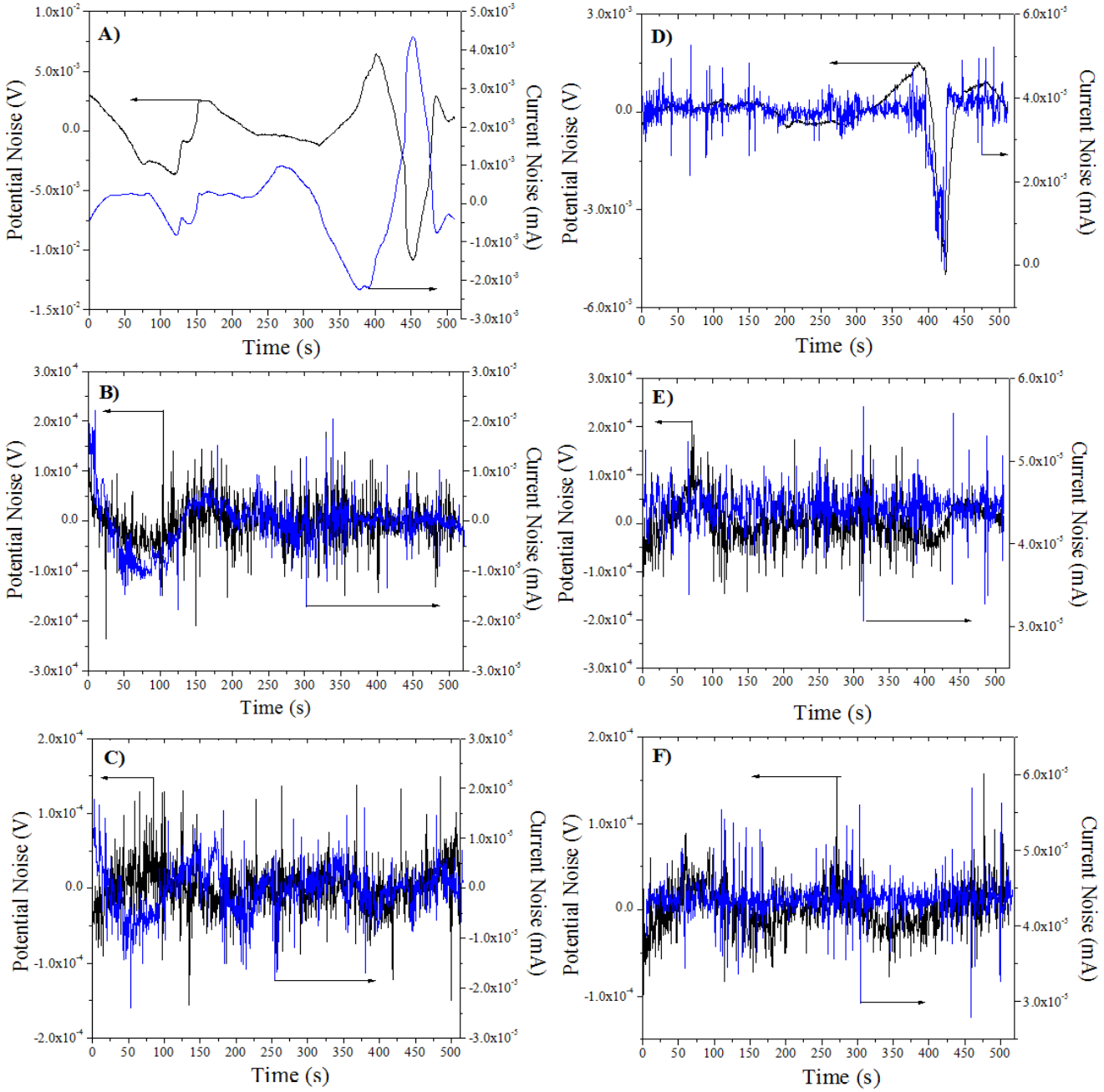

Figure 5. Time series for SS304 in $FeCl_3$: A)1 hr, B) 12 hr, C) 24 hr and NaCl: D)1 hr, E) 12 hr, F) 24 hr.

Time Series in potential and current, corresponding with 1, 12 and 24 hours are shown in Figure 5. All the data have been treated with wavelet transform to remove DC trend. In Figure 5 A), Time Series of $FeCl_3$ shows a great transient at 450 seconds, related with a decrease in the potential, and that is correlated with pitting corrosion at WE1 working electrode. However, figure 5D) for NaCl reported several fluctuations of short time duration in the first seconds of the exposition, which may be related with a metastable pitting, and at 425 seconds was observed a longer duration transient that it has the same direction as the potential signal; this behavior is attributed to a local process, occurring at

WE2 working electrode. Similar localized corrosion process for $FeCl_3$ was reported in reference [25] where the transients form are similar, however, the values in amplitude change because these have a different magnitude around of 1.0 x 10^{-1} mA, as a consequent to the $FeCl_3$ concentration differences; being lower (0.05 M) in the reference [25]. So that the activity of the ions has a big effect in the magnitude of the current noise. Time series corresponding with 12 and 24 hours in $FeCl_3$ Figure 5B) and C) and E), F) for NaCl develop a group of transients of short time duration (< 2 seconds); this behavior correspond with the metastable pitting process.

In order to determine the time and the frequency of each transient, the signal decomposition by wavelet transform is presented using the two-dimensional diagram; this kind of representation shows the total of points recorded in time (axis "x") and the frequency of scale (axis "y"). Each rectangle contains the wavelet coefficient correlated with the original signal, and the quantity in value is represented with a color in gray scale indicating from a minimum to a maximum (black to white). In this context, the two-dimensional diagram for signal noise in current of each time series from figure 5 are shown in Figure 6.

In this representation, most of the energy in the 1 hour for $FeCl_3$ (A) and NaCl (B) are concentrated in scales d_6, d_7 and d_8 and according with the shape in the transcient observed in the time series A) in Figure 5. According to Shahidi and collaborator [26] the time scale and frequency correspond with localized corrosion, produced at frequency below of 0.0625 Hz, however, with the 12 and 24 hours was observed a change in the distribution of energy from both solution since the crystals d_3, d_4 and d_5 contains a small part of the energy, this fraction correspond to high frequencies (0.0625 Hz ~ 0.5 Hz) that are reported to uniform corrosion. In this part exist a controversy because the shape of time series indicate that the transients are characteristic for metastable pitting but the number of transients generated suggest that several zones are active on the metal surface suffering oxidation and which is relating with general corrosion, therefore it´s necessary to obtain an average of the energy on each scale (EDP) that will allow to know which mechanism has more weight in these chlorine means.

The EDP of SS304 for both solution is illustrated in Figure 7 where the case for $FeCl_3$, the first hour shows a maximum of the relative energy ubicated in the d_8 following by d_7 crystal, this is related to the largest time scale which correspond with the transient from the time series in Figure 5A). The duration of this transient was more than 32 seconds, but as the time progress, at 12'th hour the behavior of the energy change to d_1 crystal with a low persistence in d_8 and d_7. The predominant mechanism in small scale was related to uniform corrosion due to the quantity of transients even if each one is related with a metastable pitting; finally, at 24 hour only d_1 predominates. At first hour in Figure 7 B), NaCl exhibit the same behavior as $FeCl_3$ however, at 12 hour there is a competition between the d_1 and d_8 crystals, this may be related with pits formation than increase the velocity of the general mechanisms. At 24 hour the tendency of the relative energy only persists in d_1 crystal for both solutions. s_8 crystal is related to the DC trend which has been removed, therefore this coefficient is shown with a value near zero in Figure 7A) and B).

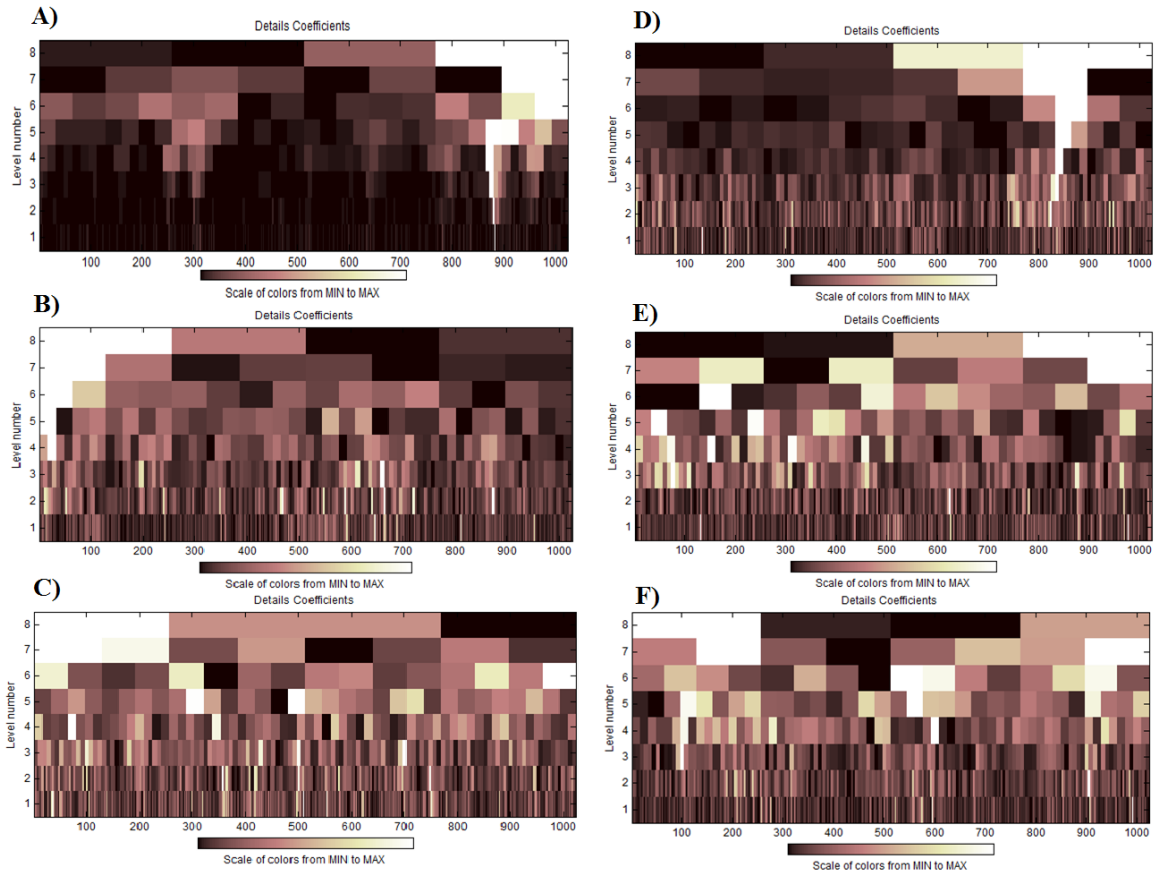

Figure 6. Two-Dimensional Representation of the coefficients of electrochemical noise current signal for SS304 in $FeCl_3$: A)1 hr, B) 12 hr, C) 24 hr; and NaCl: D)1 hr, E) 12 hr, and F) 24 hr.

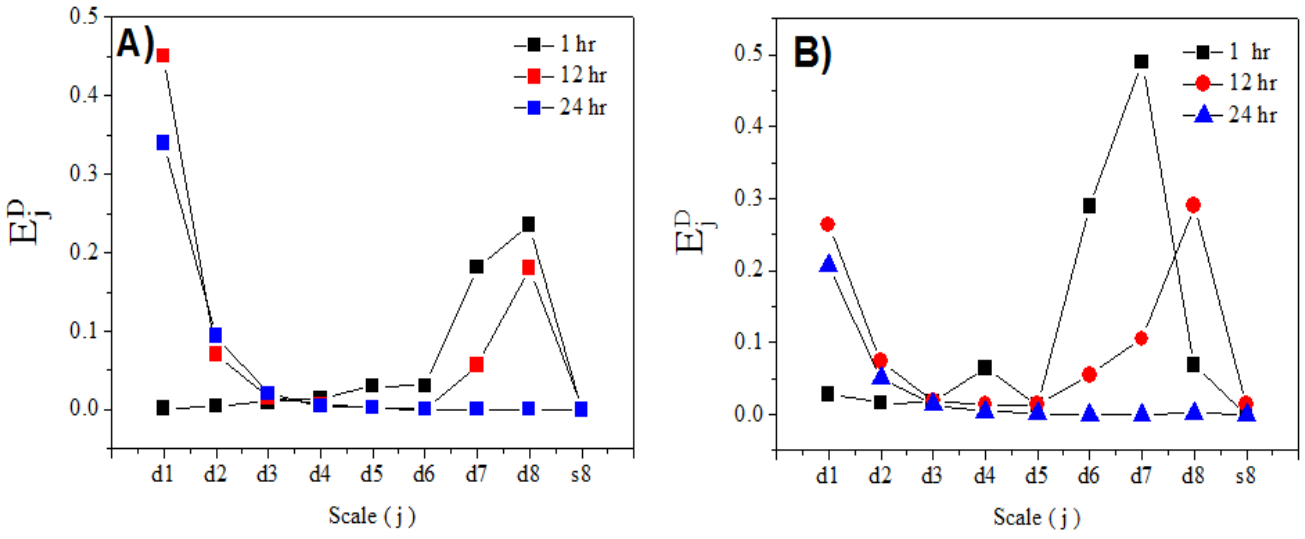

Figure 7. EDP Representation of electrochemical noise current signal for 304 in A) $FeCl_3$ and B)NaCl.

Two representation of corrosion behavior in Figure 8, were built using the parameters of shot noise theory. Here the impedance of noise Z_n was plotted in axis "y" while q, and f_n were plotted in axis "x". In plot A) the maximum characteristic frequency for NaCl is reached arround $1x10^3$ while there is a minimun that characterize to $FeCl_3$, $1x10^{-3}$; remember, that f_n is related to the corrosion

rate of the phenomenon but not to the frequency that produces a transient as demonstrated in the wavelet decomposition, that´s why to a greater degree of occurrence of the transients, the greater corrosion rate will be, this is according with Cottis [21].

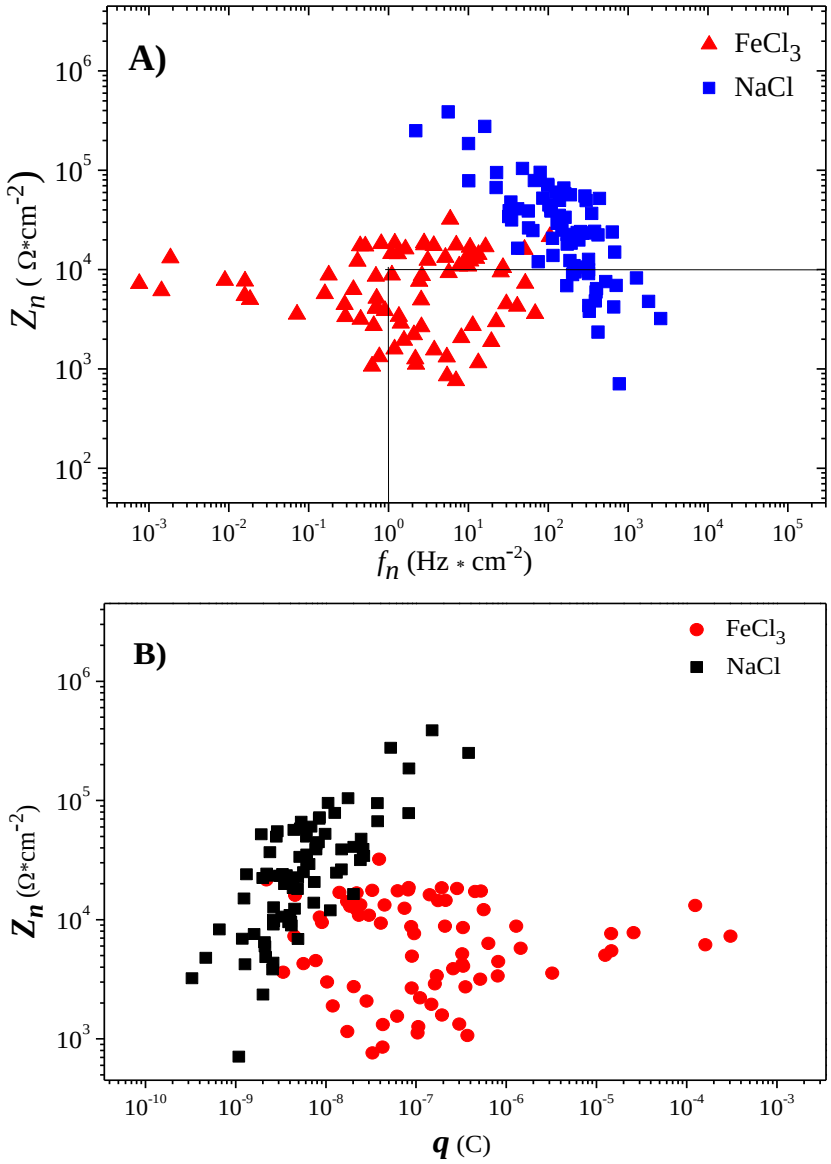

Figure 8. Corrosion behavior plots of SS304. A) Z_n vs f_n and B) Z_n vs q

Hence, those points that coincide with a lower f_n correspond to local process while the increase of f_n the corrosion mechanism will be generalized (uniform). In the case for NaCl shows that several times series are located in high characteristic frequency $1x10^1$ because most of the behavior observed in times series was thanks the presence of a great numbers of transients, that means that SS304 in NaCl (0.6 M/l), is always attacked by big number of metastables pits. In comparation with Figure 8A), the Figure 8B) is most representative of the material lost, here we can see that the SS304 in NaCl has the lowest charge transferred compared with $FeCl_3$ which has a big charge transfer in the range of $1x\ 10^{-5}$

and 1 x 10^{-4} , this points are related with the first transients formed at the start of the exposition. Finally the behavior of Z_n is correlated with the behavior of resistance (Figure 4) for both solutions.

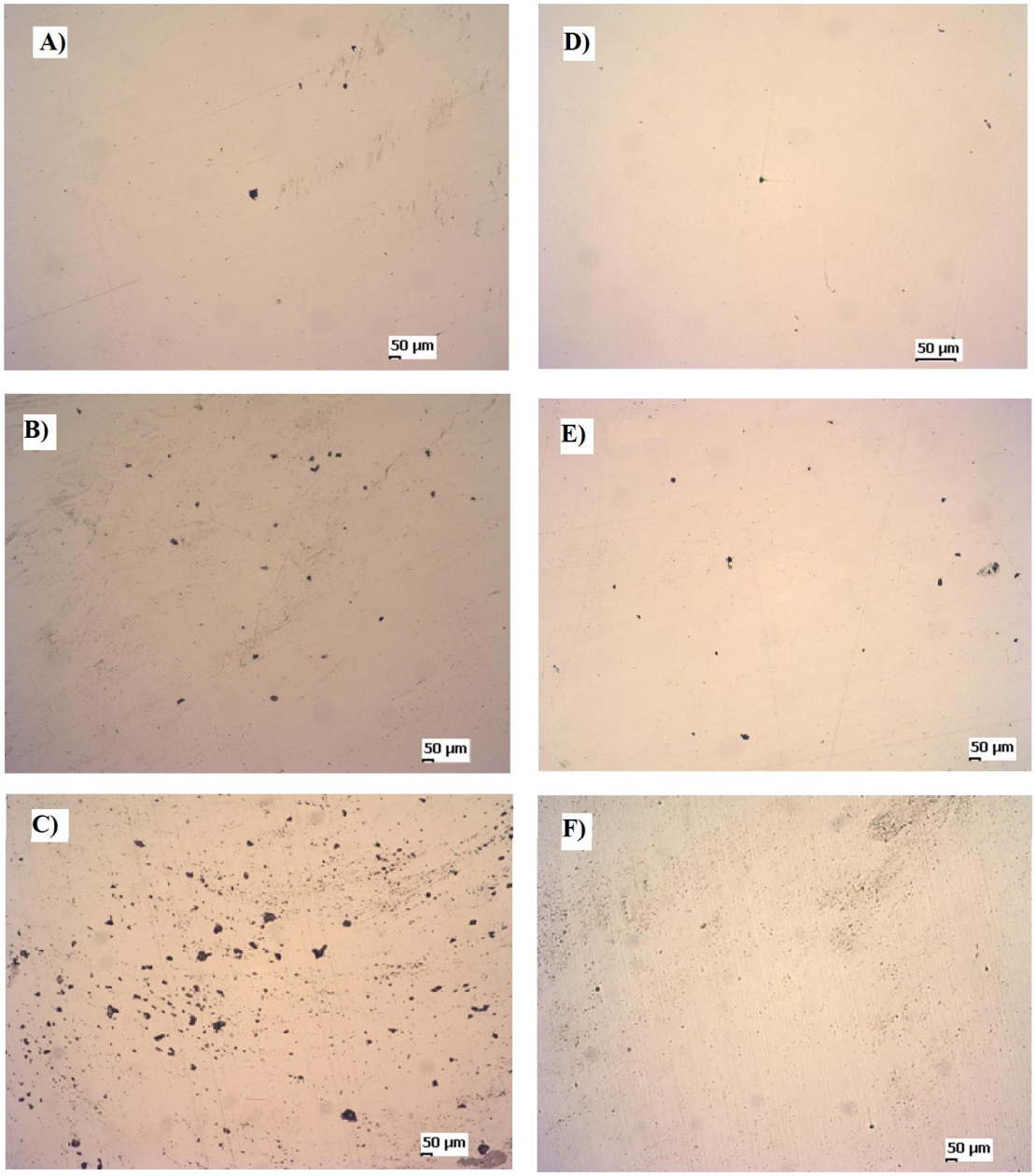

Figure 9. Metallographic of SS304 exposed in $FeCl_3$; A) 1hr, B)12 hr, C)24 hr and NaCl; D) 1hr, E)12 hr, F)24 hr.

Metallographic evidence of the corrosion mechanism is shown in Figure 9, the optical metallographic was taken according with the times selected for this research-paper. After the first hour figure A) and D) shows the formation of pits in both solution, observed more pitting density in $FeCl_3$ with an average size oscillating between 13 and 27µm in radius. According with the time series only one transient was detected, thereby, we may suggest that formation of this pitting density contribute to the total of the charge transferred during the formation of the transient, supporting the theory that

several mechanisms can be overlapping in the formation of a transient in EN signals. After 12 hours, several pits are formed homogenously in both solution B) and E) with a change in color around the pits, corresponding with the general corrosion process. At 24 hours C) and F) was observed the pits grow in number and size (max in radius >40μm), existing a coexistence with the two phenomenon, pitting and general corrosion.

4. CONCLUSIONS

The parameters of shot noise theory are reported for SS304 in two chloride solutions (NaCl and $FeCl_3$) in this experimentation. The behavior of the event charge q and the characteristic frequency f_n have demonstrated being good parameters to identify the start of the pitting process, and even, can differentiate the degree of aggressiveness and corrosion rate between the two solutions.

The impedance of noise Z_n, was in correspondence with the magnitude range of in R_p and R_n in order to prove the viability of the EN with respect the traditional techniques.

Corrosion behavior using the methodology proposed, identified two mechanisms (pitting and general corrosion) that are competing in both solutions in function of exposition time, however, it´s evident that pitting was constantly re passivating according with the data in time series and visual inspection. The values of the frequencies found during the wavelet decomposition together with the energy distribution plots, demonstrated that the predominant corrosion type after 24 h was generalized for both chloride solutions. EDP can function like a fingerprint of the predominant corrosion types.

ACKNOWLEDGEMENTS
The authors thanks to the Center of Research and Technological Development in Electrochemistry, S.C. (CIDETEQ) who supported this research with the scholarship conceded by the National Commission on Science and Technology (CONACYT). Also, thanks to the Autonomous University of the Mexican State (UAEM) for the research project conducted in CU UAEM Valle de Mexico (Laboratory of Electrochemical and Corrosion of industrial materials).

References

1. V. A. Tyagai, N. B. Lukyanchikova, *Russ. J. Electrochem*., 3 (1967) 316-322.
2. V. A. Tyagai, *Russ. J. Electrochem*., 10 (1974) 3-24.
3. C. A. Loto, *Int. J. Electrochem Sci*., 7 (2012) 9248-9270.
4. A. Legat, V. Dolecek, *Corros. Sci*., 51 (1995) 295-300.
5. G. S. Frankel, L. Stockert, F. Hunkeler, H. Boehni, *NACE*, 7 (1987) 429-438.
6. T. Zhang, D. Wang, Y. Shao, G. Meg, F. Wang, *Corros. Sci*., 58 (2012) 202-210.
7. R. M. Souto, G. T. Burstein, *Mater. Sci*., (1998) 799-806.
8. U. Bertocci, J. Kruger, *Surf. Sci.,* 101 (1980) 608-618.
9. Y. J. Tan, S. Bailey, B. Kinsella, *Corros. Sci*., 38 (1996) 1681-1695.
10. B. Li, J. Wang, X. Wang, X. Yue, *Int. J. Electrochem. Sci*., 11 (2015) 1-13.
11. A. Aballe, M. Bethencourt, F. J. B. Pedemonte, M. M. Bárcenas, *Electrochim. Acta*, 46 (1999) 4805-4816.
12. M. G. Duran, D. D. Macdonald, *Corros. Sci*., 48 (2006) 1608-1622.

13. M. Bethencourt, F. J. B. Pedemonte, M. M. Bárcenas, *Rev. Metal*., 35 (1999) 384-391.
14. S. Ritter, H. P. Seifert, Werkst. Korros., 64 (2013) 683-690.
15. M. Breimesser, S. Ritter, H. P. Seifert, T. Suter, S. Virtanem, *Corros. Sci*., 63 (2012) 129-139.
16. M. Leban, A. Legat, V. Dolecek, V. Kuhar, *Mater. Sci*., (1998) p. 157-162.
17. R.A. Cottis, M. A. Al- Ansari, G. Bagley, A Pettiti, *Mater. Sci.*, (1998) 741-754.
18. D. H. Xia, S. Song, J. Wang, J. Shi, H. Bi, Z. Gao, *Electrochem. Commun*., 15 (2012) 88-92.
19. D. H. Xia, S. Z. Song, Y. Behnamian, *Corros. Eng. Sci. Tech*., (2015)1-18.
20. R. A. Cottis, *Electrochem. Soc. Proc*., 22 (2001) 254-263.
21. H.A. Mazeedi, R.A. Cottis, *Electrochim. Acta*, 49 (2004) 2787-2793.
22. H. A. Mazeedi, R. A. Cottis, *NACE*, (2004) 1-10.
23. R. A. Cottis, J. M. S. Amaya, F. J. B. Pedemonte, *Corros Sci*., 47 (2005) 3280-3299.
24. L. Jian, Z. Huanjun, W. Ke, W. Xuehui, *Int. J. Electrochem. Sci.,* 10 (2015) 931-937.
25. G. Suresh, K. Mudali, *Corros. Sci*., 70 (2014) 238-293.
26. M. Shahidi, S. M. Hosseini, H. A. Jafari, *Electrochim. Acta*, 56 (2011) 9986-9997.